Differential behavior of NF-κB, IκBα and EGFR during the renal carcinogenic process in an experimental model *in vivo*

TELMA PARIENTE-PÉREZ[1], FRANCISCO AGUILAR-ALONSO[1], JOSÉ DOLORES SOLANO[1], CHABETTY VARGAS-OLVERA[1], PATRICIA CURIEL-MUÑIZ[1], CARMEN ADRIANA MENDOZA-RODRÍGUEZ[2], DANIELA TENORIO-HERNÁNDEZ[1] and MARÍA ELENA IBARRA-RUBIO[1]

Biology Department, Faculty of Chemistry, Laboratories [1]F-225 and [2]F-323, National Autonomous University of Mexico, CDMX 04510, Mexico

Received July 9, 2019; Accepted December 3, 2019

DOI: 10.3892/ol.2020.11436

Abstract. Renal cell carcinoma (RCC) is the most common type of cancer of the adult kidney. It is generally asymptomatic even at advanced stages, so opportune diagnosis is rare, making it almost impossible to study this cancer at its early stages. RCC tumors induced by ferric nitrilotriacetate (FeNTA) in rats histologically correspond to the human clear cell RCC subtype (ccRCC) and the exposure to this carcinogen during either one or two months leads to different early stages of neoplastic development. High levels of nuclear factor kappa B (NF-κB) and epidermal growth factor receptor (EGFR) as well as low levels of NF-κB inhibitor alpha (IκBα) are frequent in human RCC, but their status in FeNTA-induced tumors and their evolution along renal carcinogenesis is unclear. On this basis, in the present study NF-κB, IκBα and EGFR behavior was analyzed at different stages of the experimental renal carcinogenesis model. Similar to patients with RCC, neoplastic tissue showed high levels of p65, one of the predominant subunits of NF-κB in ccRCC and of EGFR (protein and mRNA), as well as a decrease in the levels of NF-κB's main inhibitor, IκBα, resulting in a classic oncogenic combination. Conversely, different responses were observed at early stages of carcinogenesis. After one month of FeNTA-exposure, NF-κB activity and EGFR levels augmented; but unexpectedly, IκBα also did. While after two months, NF-κB activity diminished, but EGFR and IκBα levels remained elevated. In conclusion, FeNTA-induced tumors and RCC human neoplasms are analogues regarding to the classic NF-κB, IκBα and EGFR behavior, and distinctive non-conventional combination of changes is developed at each early stage studied. The results obtained suggest that the dysregulation of the analyzed molecules could be related to different signaling pathways and therefore, to particular effects depending on the phase of the carcinogenic process.

Correspondence to: Dr María Elena Ibarra-Rubio, Biology Department, Faculty of Chemistry, Laboratory F-225, Building F, National Autonomous University of Mexico, 3000 University Av., Coyoacan, CDMX 04510, Mexico
E-mail: meir@unam.mx

Abbreviations: ccRCC, clear cell renal cell carcinoma; FeNTA, ferric nitrilotriacetate; DEN, *N*-dietilnitrosamine; DF, DEN+FeNTA; NTT, non-tumor tissue; TT, tumor tissue; AT, adjacent tissue; WB, western blotting; IHC, immunohistochemistry; EMSA, electrophoretic mobility shift assay

Key words: clear cell renal cell carcinoma, ferric nitrilotriacetate, carcinogenesis, experimental model *in vivo*, NF-κB, p65, IκBα, epidermal growth factor receptor

Introduction

Renal cell carcinoma (RCC) is the most common type of kidney cancer in adults (1). Patients are generally asymptomatic chiefly at the initial phases. Specific early markers have not been identified, resulting in a late diagnosis, frequently even when metastasis is already present (1,2), and there are different histological subtypes with distinct responses to therapies (3). All of the above lead to high mortality rates (1). Hence, an experimental model would be a valuable tool to study this disease and particularly to understand the molecular mechanisms involved in the early stages of renal carcinogenic process, which is almost impossible to achieve in patients. The authors' group has demonstrated that *N*-diethylnitrosamine (DEN)-initiated and ferric nitrilotriacetate (FeNTA)-promoted renal tumors histologically correspond to clear cell RCC (ccRCC), the most common subtype occurring in patients (4) and that the exposure to FeNTA during either one or two months, causes distinct pre-neoplastic lesions and pro-carcinogenic molecular alterations, representing these times of exposure, differential early stages of renal carcinogenesis (5,6).

Nuclear factor kappa B (NF-κB) is a collective term to refer to the family of dimeric Rel transcription factors, which consists of five proteins: p65 (Rel A), c-Rel, RelB, NFκB1 (p105/p50) and NFκB2 (p100/p52) (7), being considered p65/p50 the most classic dimer, where p65 is the subunit responsible for the transactivation of its target genes (8). In most cells, NF-κB is retained in the cytoplasm by its inhibitory protein, IκB (7,8), which blocks the factor's nuclear localization signal. IκB separation, therefore, allows NF-κB nuclear translocation and its consequent binding to κB sites in DNA. Additionally, NF-κB's

activity is controlled in the nucleus by IκB as well, where it induces the factor's liberation from chromatin and its export to the cytoplasm (9,10). The expression of numerous genes related to various events such as cell proliferation, inflammation and inhibition of apoptosis, is under the influence of this transcription factor (7), its deregulation being associated with almost all types of cancer (11,12). Particularly, different authors have reported an NF-κB overexpression in RCC tumors and cell lines (12-15), and in certain publications this overexpression has been correlated to tumor grade, invasion and metastasis, proposing the factor as a target for RCC treatment (2,3,14,16). In fact, apoptosis-induction and/or growth-repression of different RCC cell lines have been demonstrated by using a specific inhibitor of NF-κB activation (Bay-11-7085) or by blocking tyrosine kinases involved in NF-κB activation signaling (17,18). The p65 subunit was studied in all the aforementioned reports apart from Meteoglu *et al* (12) who analyzed the p50 subunit. Furthermore, Ng *et al* (19) reported a decrease in the levels of p50, p52 and c-Rel, as well as the absence of RelB, but an increase in p65 expression in human RCC tumors.

On the other hand, the epidermal growth factor receptor (EGFR) gene is a known target of NF-κB (20). The EGFR is a transmembrane protein of the ErbB tyrosine kinases family (21) and when it is activated, multiple signaling pathways are induced, thus modulating pleiotropic cell responses, such as proliferation, migration and apoptosis (21). In the kidney, this receptor participates in renal hemodynamics, electrolyte management, magnesium reabsorption, phosphate transport regulation and proximal tubule gluconeogenesis, as well as in renal reparation after ischemia-induced damage (22). However, dysregulation of EGFR has been associated with progressive fibrotic renal damage, polycystic renal disease and RCC (22). In this last case, previous studies have reported EGFR overexpression, but the clinical significance of this increase and its subcellular localization are still controversial (23-28).

Therefore, in the present study, the behavior of NF-κB (p65), IκBα and EGFR was analyzed in renal tumors and at different early stages of FeNTA-induced carcinogenesis, to establish the equivalence between experimental and human neoplasms in this regard and to investigate the probable participation of these molecules in RCC development.

Materials and methods

Reagents and antibodies. All reagents were purchased from Sigma-Aldrich Merck KGaA unless otherwise indicated. Primary antibodies against IκBα (cat. no. sc-371), NF-κB p65 (cat. no. sc-8008), EGFR (cat. no. sc-03-G), α-tubulin (cat. no. sc-5286), GAPDH (cat. no. sc-48167), β-actin (cat. no. sc-1616) and histone H3 (cat. no. sc-10809) used for western blotting (WB), immunohistochemistry (IHC), and the supershift test of the electrophoretic mobility shift assay (EMSA), as well as the secondary antibodies (anti-mouse and anti-rabbit, cat. nos. sc-2005 and sc-2004, respectively) used for WB were purchased from Santa Cruz Biotechnology, Inc., while the anti-IgG secondary antibodies coupled with biotin (ABC kit Vectastain®; cat. nos. PK-6101 and PK 6102) and the peroxidase substrate kit DAB (cat. no. SK-4100) used for IHC were purchased from Vector Laboratories, Inc.

Carcinogen preparation. FeNTA solution was prepared as previously described (6).

Experimental protocol. All experiments involving animals were performed according to the Mexican Official Norm NOM-062-ZOO-1999 and approved by the Institutional Committee for the Use and Care of Laboratory Animals (FQ/CICUAL/081/14). Experimental protocols were carried out as previously described (6) adapted from other authors' studies (29-31). Briefly, 67 male Wistar rats aged between 31 and 36 days and weighing 70-80 g were housed in a controlled temperature environment (21-23˚C) with 55-62% humidity and under 12 h light/dark cycles. Rats had free access to food and water and were randomly distributed in two groups: 18 animals treated with a vehicle were used as the control group (C) and 49 animals treated with a single intraperitoneal (i.p.) administration of *N*-DEN (200 mg_{DEN}/kg_{bw}) and weekly increasing i.p. doses of FeNTA (3-9 mg_{Fe}/kg_{bw}) twice a week, maintaining the 9 mg_{Fe}/kg_{bw} dose from the 4th to the 16th week in the carcinogenesis group (DF). To analyze early stages of carcinogenesis, 10 rats were decapitated after one month and 10 more after two months of FeNTA-exposure for DF group as well as 6 animals for the corresponding C group for each time of study. Euthanasia was executed, in both cases, 48 h after the last injection of the carcinogen to avoid its acute effects and without anesthesia as the anesthetic may interfere in different manners with the chemistry of renal tissue and other tissues of interest, such as liver and brain, as well as blood samples. In the present study specifically kidneys, liver and lungs were used. Organs were removed immediately after sacrifice. The renal cortex was carefully dissected and all tissues were immediately frozen in liquid nitrogen storing them at -70˚C until use. For the carcinogenesis protocol, the remaining animals were euthanized two months after the final FeNTA exposure, some of them by decapitation as described above to obtain tumor samples for reverse transcription (RT)-PCR assays, while others were anesthetized i.p. with sodium pentobarbital (50 mg/kg_{bw}) and the kidneys were perfused with pH 7.4 Krebs-Ringer solution with 250 mM ethylendiaminetetraacetic acid (EDTA), formalin-fixed at room temperature for 24 h and prepared for IHC following standard protocols (32). Animal welfare was carefully monitored during the experimental protocol, twice a week during the first 3 months and 4 times a week during the last three months. Euthanasia was executed by carbon dioxide inhalation when rats showed signs of health deterioration such as loosing 20% of weight, or exhibiting prostration, mobility impairment and/or difficulty eating, urinating or defecating.

IHC. Sections (5-μm thick; rotation micrometer, Leica®; Leica Microsystems GmbH) from formalin-fixed paraffin-embedded kidney tissue specimens were placed on slides, deparaffinized with xylene and rehydrated with decreasing concentrations of ethanol (100, 96, 80, 70 and 50%) for 3 min each. The antigen was retrieved by heating at 100˚C for 30 min in 0.01 M sodium citrate buffer (pH 6.0) and subsequently incubated for 30 min with blocking solution (3% H_2O_2 in PBS) to suppress the endogenous peroxidase activity. After rinsing with PBS, the slides were incubated in 0.5% Triton X-100 at room temperature for 30 min and non-specific immunoglobulin binding was blocked

by incubating sections in 5% albumin IgG free (Jackson ImmunoResearch Laboratories, Inc.) in PBS at room temperature for 30 min. The slides were incubated overnight at 4˚C in a humidified chamber with the corresponding primary antibody at a 1:250 dilution, prepared with 3% Triton X-100 in PBS. Then, the unbound primary antibody was removed by washing with PBS and the slides were incubated at room temperature for 2 h with a 1:200 dilution of anti-rabbit or anti-mouse (case dependent) IgG secondary antibody coupled with biotin (ABC kit Vectastain®, Vector Laboratories, Inc.). Sections were washed with PBS and incubated for 1 h at room temperature in peroxidase-conjugated avidin-biotin reagent (ABC kit Vectastain®, Vector Laboratories, Inc.). The immunoreaction was detected with the DAB kit (Vector Laboratories Inc.) and samples were counterstained with hematoxylin at room temperature for 2 min and dehydrated with increasing concentrations of ethanol (50, 70, 80, 96 and 100%), and solutions of 1:1 ethanol-xylene and 100% xylene for 3 min each. Finally, four random fields of each sample were analyzed utilizing a Nikon E600 light microscope; the staining intensity (mean grey value) of immunopositive cells was evaluated with the ImageJ software version 1.44p (National Institutes of Health) (33), which converts the grey level to a numerical value using a scale from 0 (white) to 255 (black), as described previously (32).

mRNA extraction and RT-PCR. Semi-quantitative mRNA analysis was achieved by RT-PCR. Total RNA was extracted with the Direct-zol™ RNA MiniPrep kit according to the manufacturer's protocol (cat. no. R2052, Zymo Research). RNA concentrations were determined spectrophotometrically at 260 nm. RT-PCR was carried out starting with 1 μg of total RNA following manufacturer's protocol with the RevertAid First Strand cDNA Synthesis kit (cat. no. K1622; Thermo Fisher Scientific, Inc.). The thermocycling conditions for cDNA synthesis and amplification were: 1 cycle 55˚C (30 min), 94˚C (2 min), 94˚C (30 sec); 10 cycles 94˚C (30 sec), 60˚C (30 sec), 72˚C (30 sec); 20 cycles 94˚C (30 sec), 60˚C (30 sec), 72˚C (5-30 sec with five seconds increases per cycle); 1 cycle 94˚C (30 sec), 60˚C (30 sec) and 72˚C (7 min). GAPDH was used as control. The oligonucleotide sequences used were: (1) for EGFR, 5'-ACAGAGGACAACATAGATGAC-3' (forward) and 5'-CTGGGCAGTGTTGAGATAC-3' (reverse) (34); and (2) for GAPDH, 5'-GGCTGAGAATGGGAAGCTGGT CAT-3' (forward) and 5'-CAGCCTTCTCCATGGTGGTGA AGA-3' (reverse) (35). Amplified fragments were analyzed on a 2% agarose gel stained with ethidium bromide at room temperature for 30 min and visualized with ultraviolet light (Benchtop 2UV™ Transilluminator UVP). Bands were quantified by densitometry analysis as described below.

Tissue homogenates and western blot analysis. A total of 150 mg of renal cortex tissue were homogenized (PT10/35GT homogenizer Polytron®; Kinematica AG), in cold lysis buffer (1 mM DTT, 10 mM Tris-HCl, 1 mM EDTA, 1 mM sodium orthovanadate, 15 mM sodium azide, 1.0% Triton X-100 and 30% glycerol) supplemented with the commercial protease inhibitor cOmplete™ Mini and phosphatase inhibitor PhosSTOP™ Cocktail tablets (Roche Diagnostics GmbH). After homogenates' centrifugation (13,000 x g for 30 min at 4˚C) (Thermo Fisher Scientific, Inc.; Legend RT+ centrifuge), supernatants were recovered and total protein was quantified by the Bradford method (Bio-Rad Laboratories Inc.). Equal protein amounts (60-80 μg) were electrophoresed in a 10% SDS-PAGE polyacrylamide gel and transferred to an Immobilon® PVDF membrane (EMD Millipore). Membranes were blocked for 1 h at room temperature with 1% nonfat dry milk and incubated with the primary antibodies against p65 (1:250), IκBα (1:250), EGFR (1:250) or α-tubulin (1:1,000) overnight at 4˚C. Subsequently, membranes were washed and incubated with the corresponding secondary antibody (1:30,000 for anti-rabbit and anti-mouse). Immunoreactive signal bands were detected using Immobilon™ Western Chemiluminescent HRP Substrate (EMD Millipore) and were recorded on X-ray films and quantified by densitometry, as described below.

Nuclear protein extraction and EMSA. Nuclear protein extracts were prepared by homogenizing 100 mg kidney cortex (PT10/35GT homogenizer Polytron® Kinematica AG) for 8-20 sec in 800 μl buffer A (10 mM HEPES, pH 7.9, 1.5 mM $MgCl_2$, 10 mM KCl, 0.5 mM DTT, 0.5 mM PMSF and a tablet of protease inhibitor cOmplete™ Mini per 10 ml buffer). Homogenates were mixed with 5 μl Nonidet P-40 (NP-40) and incubated at 4˚C for 20 min, stirring 10 times at intervals of 2 min. Then samples were centrifuged for 15 min at 1,500 x g at 4˚C (Thermo Fisher Scientific, Inc.; Legend RT+ centrifuge) and pellets were resuspended in 100 μl buffer B (20 mM HEPES, pH 7.9, 420 mM NaCl, 25% glycerol, 1.5 mM $MgCl_2$, 0.2 mM EDTA, 0.5 mM PMSF, 0.5 mM DTT and a tablet of protease inhibitor cOmplete™ Mini for each 10 ml buffer). After 20 min of incubation at 4˚C, mixing by inversion every 2 min, tubes were centrifuged for 10 min at 13,000 x g at 4˚C (Thermo Fisher Scientific, Inc.; Legend RT+ centrifuge) and the supernatants containing the nuclear proteins were stored at -20˚C until use. EMSA assay and oligonucleotide digoxigenin labeling were carried out using a commercial kit according to manufacturer's protocol (DIG Gel Shift kit, 2nd generation, Roche Diagnostics GmbH). Briefly, 60 μg of nuclear proteins were incubated with 2 ng of labeled double-stranded consensus sequence recognized by NF-κB: 5'-AGTTGAGACTTTCCC GGGAGGC-3' (Santa Cruz Biotechnology, Inc.). DNA-protein complexes were resolved by 5% native polyacrylamide gel electrophoresis with 0.5X TBE (50 mM Tris, 45 mM boric acid and 0.5 mM EDTA) for 120 min at 80 V. Samples were transferred to a positively-charged nylon membrane (Roche Diagnostics GmbH) in 0.5X TBE for 30 min at 300 mA (Trans-Blot® SD Semi-dry Transfer cell, Bio-Rad Laboratories Inc.) and crosslinked for 60 sec (CL-1000 Ultraviolet Crosslinker, UVP). Finally, digoxigenin immunodetection was performed and autoradiographs developed. The specificity of binding and recognition of the shifted-bands' identity was examined by: i) Assays without sample, ii) assay without labeled oligonucleotide, iii) competition assay with 100-fold molar excess of unlabeled oligonucleotide and iv) supershift assay performed by previously incubating the nuclear extract with the anti-p65 antibody for 15 min at 37˚C.

Cell fractionation. A total of 150 mg of renal cortex were homogenized (PT10/35GT homogenizer Polytron® Kinematica) in Gough buffer (10 mM Tris-HCl, 0.15 M NaCl, 1.5 mM $MgCl_2$,

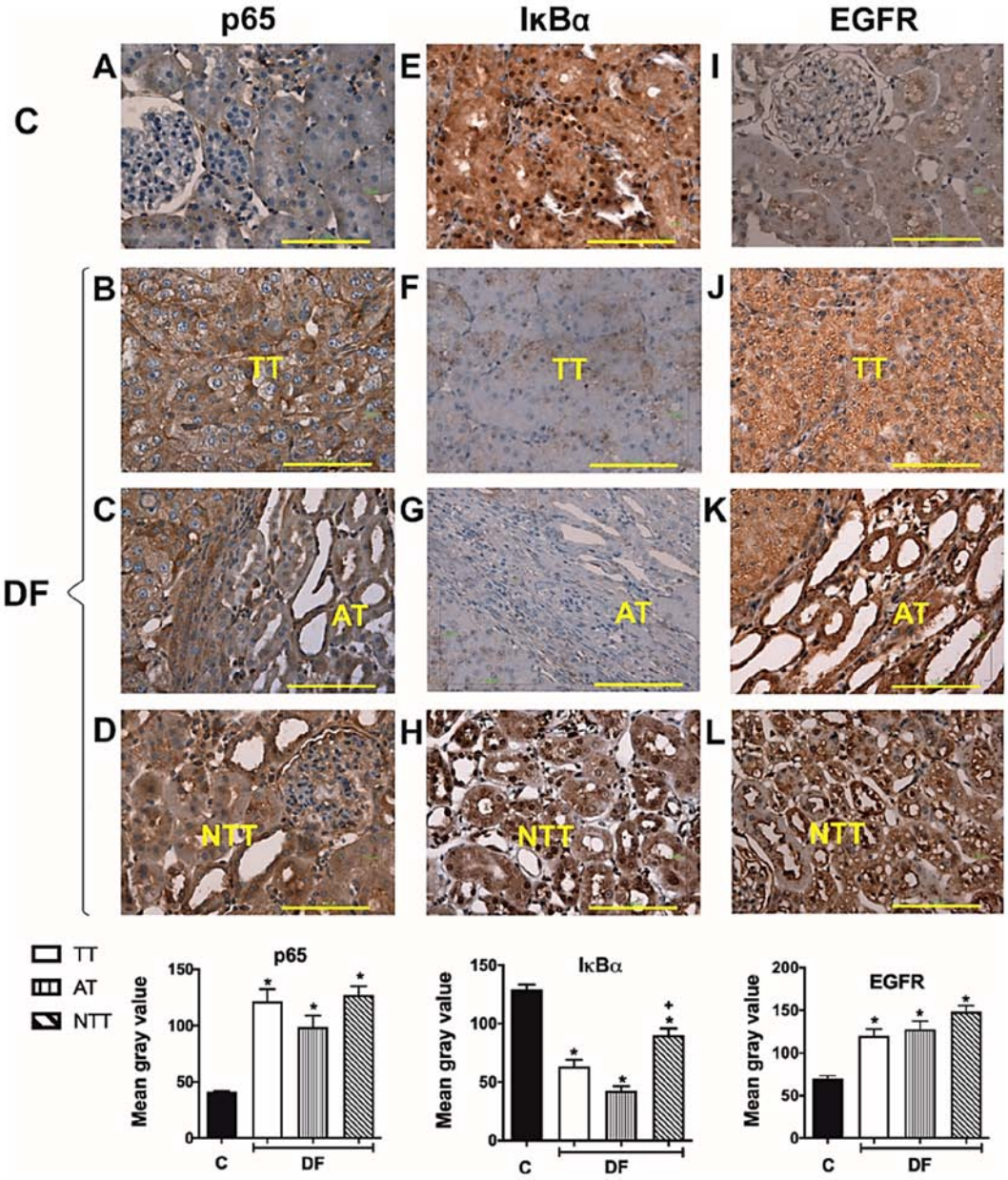

Figure 1. Immunohistochemistry of NF-κB (p65), IκBα and EGFR in renal samples obtained at the end of the carcinogenesis protocol. (A-L) Representative kidney cortex photomicrographs of these proteins are displayed from the C group for (A) p65, (E) IκBα and (I) EGFR and DF exposed rats, as well as the corresponding quantification histograms. NF-κB (p65) levels increased (B) TT, (C) AT and (D) NTT in a similar way. IκBα levels were abated in (F) TT, (G) AT and (H) NTT regions in the DF group, although in this case the decrease in NTT was smaller than in TT and AT. For its part, low EGFR expression in C rats was observed, (I) which increased in kidneys from the DF group in the analyzed areas in a comparable manner for (J) TT, (K) AT, and (L) NTT. AT images (C, G and K) include a TT area as reference. Scale bar=100 μm. Magnification, x400. A total of four random fields per sample were analyzed, n=3 for the C group and 5 for the different areas of DF group. Results are expressed as the mean gray value. Columns represent the mean ± standard error of the mean. *P≤0.05 vs. C, $^{+}$P≤0.05 vs. TT and AT. C, control group; DF, N-dietilnitrosamine + ferric nitrilotriacetate treated group; TT, tumor tissues; AT, adjacent tissue; NTT, non-tumor tissue; NF-κB, nuclear factor kappa B; EGFR, epidermal growth factor receptor.

0.65% NP-40, 0.5 mM PMSF and 1 mM DTT) and incubated on ice for 30 min with agitation every 5 min. Homogenates were centrifuged at 13,000 x g for 2 min at 4˚C (Thermo Fisher Scientific, Inc.; Legend RT+ centrifuge). Supernatants (cytoplasmic fraction) were recovered and stored at 4˚C and pellets were resuspended in 250 μl HEPES buffer (20 mM HEPES, pH 7.9, 25% glycerol, 0.4 M NaCl, 1.5 mM $MgCl_2$, 0.2 mM EDTA, 0.5 mM PMSF and 1 mM DTT). After 2 h of incubation at 4˚C with constant agitation, samples were centrifuged for 10 min at 12,000 x g at 4˚C (Thermo Fisher Scientific, Inc.; Legend RT+ centrifuge) and supernatants (nuclear proteins) were transferred to tubes containing 400 μl buffer D (20 mM HEPES, pH 7.9, 20% glycerol, 50 M KCl, 0.2 M EDTA, 0.5 mM PMSF and 1 mM DTT). Protein concentrations were determined by the Bradford method (Bio-Rad Laboratories Inc.) to load the same amount of protein from the cytoplasmic and nuclear fractions in electrophoresis gels for WB analysis.

Densitometry and statistical analysis. Densitometry analysis was performed using the ImageJ Software version 1.44p (NIH) (33). For WB and RT-PCR, the results from the experimental groups were expressed as relative densitometric units

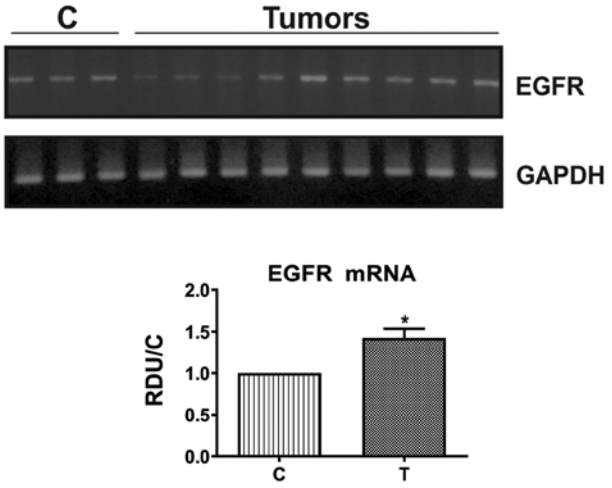

Figure 2. EGFR mRNA levels in ferric nitrilotriacetate (FeNTA)-induced tumors. Representative images of ethidium bromide stained agarose gel electrophoresis of EGFR and GAPDH cDNAs obtained by reverse transcription-PCR, as well as a histogram of the densitometry analysis of all samples assayed are shown. The mean value of EGFR mRNA levels showed an increase, but its behavior varied among the tumors analyzed; while some of them exhibited an increase, others presented a reduction or had no changes. Bars represent the mean ± standard error of the mean. n=5 for C group and 14 for tumors. *P≤0.05 vs. C. RDU, relative densitometric units vs. GAPDH and with respect to the C group; EGFR, epidermal growth factor; C, control.

with respect to the control group (RDU/C), calculated by dividing the total densitometric arbitrary units of each band corresponding to the protein of interest, by the value of the band corresponding to the protein used as loading control, obtained from the same sample in the same membrane; and this result, in turn, was divided by the value obtained from the control group. For EMSA, data were calculated by dividing the densitometric units of the shifted oligonucleotide band from problem samples by the mean densitometric value obtained from control samples. Lastly, for WB of cell fractions, results were expressed as the rate obtained by dividing the densitometric value of the band corresponding to the protein of interest by that of the loading control band (RDU).

All data are presented as the mean ± standard error of the mean. Results were analyzed by one-way analysis of variance followed by Tukey post hoc test on Fig. 1 and by unpaired t-test with Welch's correction in all other figures. Statistical analysis was performed using GraphPad Prism version 5.0b for Windows (GraphPad Software, Inc.). P≤0.05 was considered to indicate a statistically significant difference.

Results

p65, IκBα and EGFR in FeNTA-induced renal tumors. Initially, to determine if FeNTA-induced tumors exhibited similar alterations to those reported in human RCC, the behavior of NF-κB (p65), IκBα and EGFR was analyzed in tumor tissue (TT), as well as in adjacent tissue (AT) and non-TT (NTT) from the DF group compared with the renal cortex from the C group. Fig. 1 displays IHC representative images and histograms of the mean immunoreactivity quantification of these three molecules in renal samples from C and DF groups. Unlike renal tissue from C rats, where low NF-κB (p65) presence was detected (Fig. 1A), a strong positive NF-κB (p65) stain was observed in all kidney areas studied from the DF group (Fig. 1B-D), i.e. the increase in this protein was similar in TT, AT and NTT. In contrast, the intensity of the IκBα positive stain observed in the C group (Fig. 1E) decreased in rats exposed to the carcinogen (Fig. 1F-H). Interestingly, NTT exhibited an IκBα staining intensity that was decreased compared with the C group, but higher than the TT and AT, as well as a more frequent nuclear presence (Fig. 1H). Concerning EGFR, immunostaining was similar in TT and AT with a heterogeneous behavior, showing different levels of overexpression 63% of the studied samples (Fig. 1J) as compared with C (Fig. 1I); while 37% had no changes or even presented a negative stain. However, the mean value of EGFR levels for all analyzed specimens displayed an augment in TT as well as in AT, and it was detected preferentially in the cytoplasm in both areas; although the nuclear presence of this receptor was higher in AT. In NTT, conversely, EGFR levels increased in all samples in the cytoplasm and in the nucleus (Fig. 1L), like in AT. Moreover, in concordance with protein behavior, the mean EGFR mRNA levels were also significantly enhanced in tumors, despite some samples showing no changes or a decrease (39%) (Fig. 2).

p65, IκBα and EGFR at early stages of FeNTA-induced renal carcinogenesis. p65, IκBα and EGFR levels were determined in the kidney cortex from FeNTA-exposed rats during either one or two months, in order to study the probable participation of these molecules in the carcinogenic process. WB representative images and densitometry analysis of all samples examined are displayed on Fig. 3. Results exhibited no changes in p65 protein levels after either one or two months of FeNTA-exposure (Fig. 3A). In the case of IκBα (Fig. 3A), two bands were observed, one being present mainly in the C group with an electrophoretic shift corresponding to a molecular weight of ~32 kDa, while the other one was more intense in DF group, showing a displacement that corresponds to ~34 kDa, which is closer to the molecular weight reported for IκBα in rats, i.e. 35 kDa (Uniprot #UniRef90_P2596). Due to the above, IκBα results were calculated with the sum of the densitometric units from both bands, finding a statistical augment at both times studied, which was more evident after one month of carcinogen-exposure. On the other hand, EGFR levels were significantly enhanced in the DF group at both times studied (Fig. 3B) and, although the rise seems to be more intense after one month of FeNTA-exposure, as occurred for IκBα, there was no statistical difference between them.

NF-κB activity and EGFR mRNA expression at early stages of FeNTA-induced renal carcinogenesis. Given the preceding findings, EMSAs were carried out in nuclear extracts to investigate NF-κB-DNA binding activity (Fig. 4A). Different tests were performed as technique controls: i) Assays without sample and ii) without labeled-oligonucleotide, where no shifted band was detected (lanes 1 and 2, respectively); iii) a competition assay with a 100-fold molar excess of unlabeled-oligonucleotide, to confirm the identity of the observed band (lane 3); and vi) a supershift assay using the anti-p65 antibody to verify the presence of this protein in the NF-κB complex (lane 4). These two last tests were conducted with the

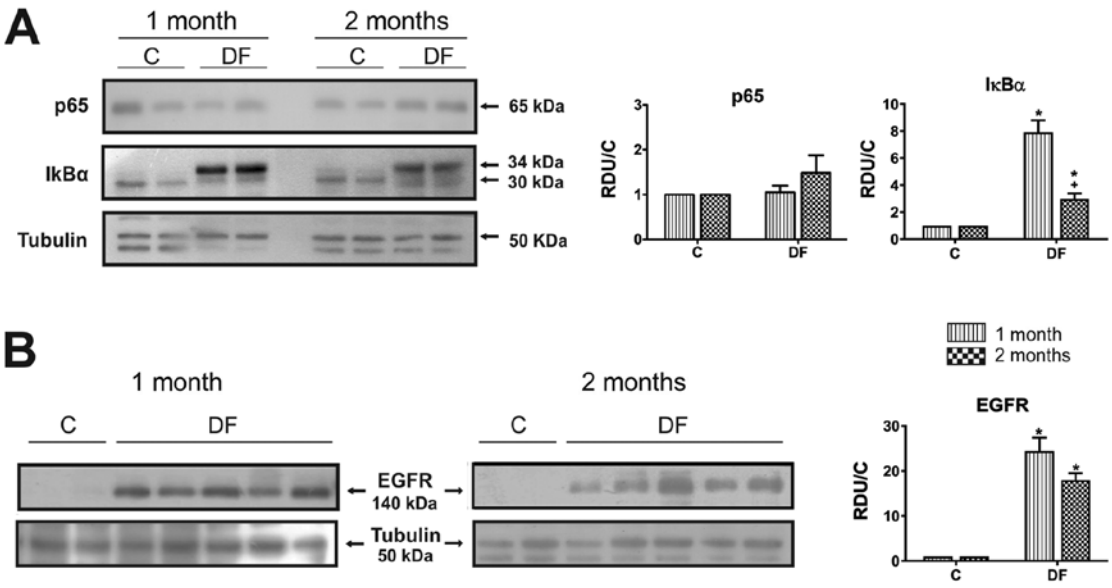

Figure 3. p65, IκBα and EGFR protein levels at early stages of FeNTA-induced renal carcinogenesis. Representative images of western blot assays and histograms are presented. (A) p65 levels did not change in the DF group with respect to C at any time studied. In contrast (A) IκBα as well as (B) EGFR increased in both stages, although to a lesser extent after two months of carcinogen-exposure than after one. α-tubulin was used as a loading control. Bars represent the mean ± standard error of the mean. n=4 for C groups and 7 for DF groups. *P≤0.05 vs. corresponding C, and +P≤0.05 vs. DF after one. C, control group; DF, N-dietilnitrosamine + FeNTA treated group; RDU, relative densitometric units vs. corresponding tubulin and with respect to the C group; EGFR, epidermal growth factor receptor.

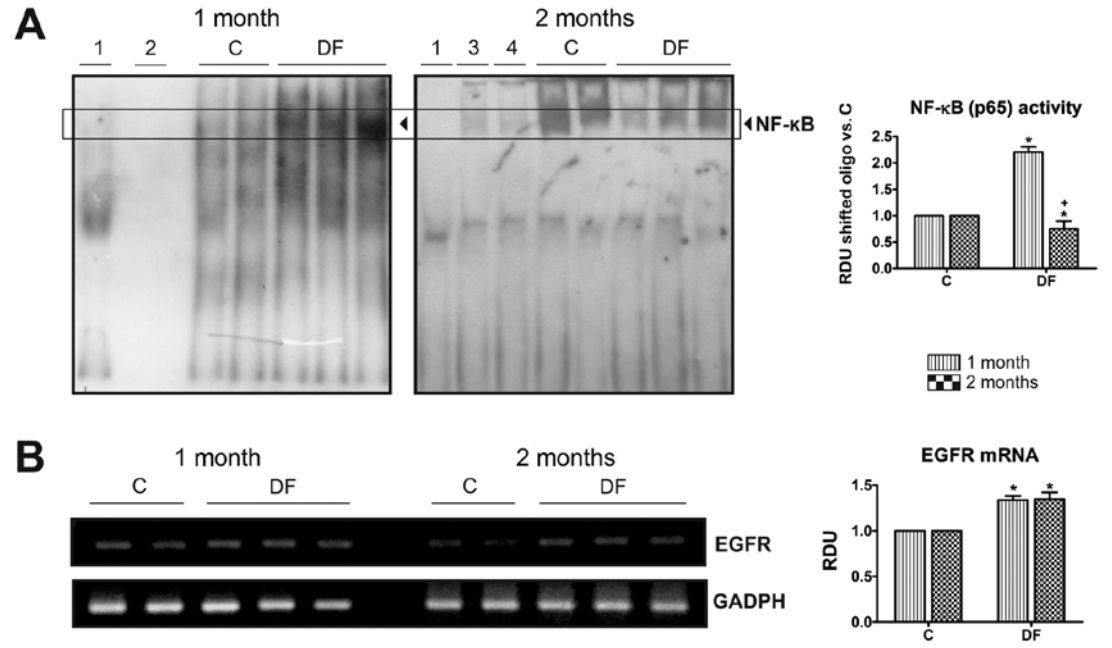

Figure 4. NF-κB activity analyzed by EMSA and EGFR mRNA levels determined by reverse transcription-PCR at early stages of FeNTA-induced renal carcinogenesis. Representative images of both determinations as well as corresponding histograms of densitometric analysis of all samples assayed are exhibited. (A) EMSAs were performed using nuclear extracts: Lane 1: Digoxigenin-labeled oligonucleotides without sample; lane 2: Sample without oligonucleotides; lane 3: Competition assay carried out using a 100-fold molar excess of unlabeled oligonucleotides; lane 4: Supershift assay performed utilizing an anti-p65 antibody. DF exposure induced an increase in NF-κB activity after one month, but it decreased after two months. (B) EGFR mRNA levels increased by a similar degree at both times of exposure. GAPDH was used as a loading control. Bars represent the mean ± standard error of the mean. n=4 for C groups and 7 for DF groups. *P≤0.05 vs. corresponding C and +P≤0.05 vs. DF after one month. C, control group; DF, N-dietilnitrosamine + FeNTA treated group; EMSA, electrophoretic mobility shift assay; RDU, relative densitometric units vs. GAPDH and with respect to the C group; NF-κB, nuclear factor kappa B; EGFR, epidermal growth factor receptor.

first control sample shown in the two months image and where a notable decrease in the intensity of the corresponding band can be appreciated. When samples were analyzed, a patent rise of NF-κB binding to its consensus sequence was observed after one month of FeNTA-exposure; whereas the factor's activity was abated after two months' exposure revealed by

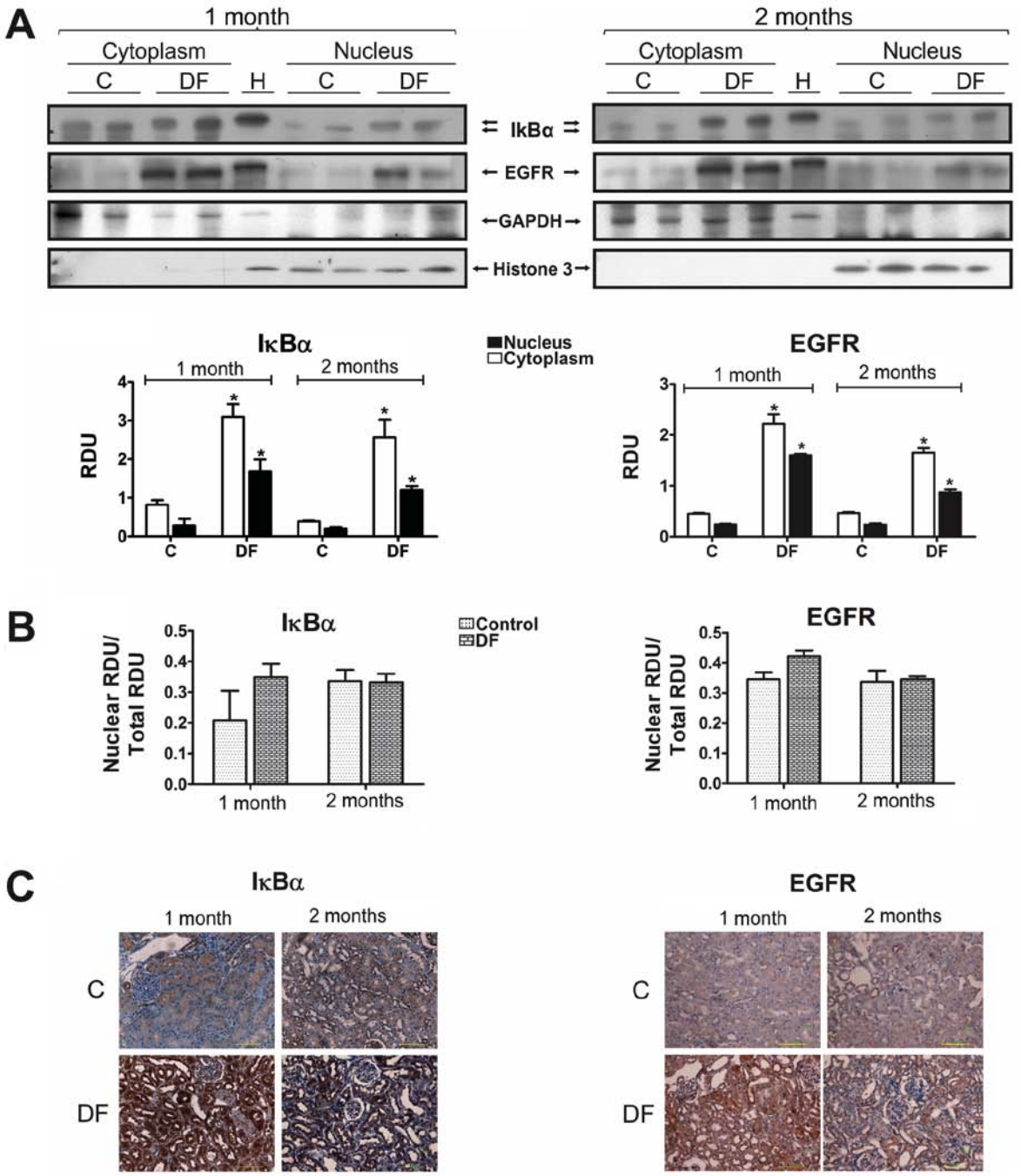

Figure 5. Subcellular distribution of IκBα and EGFR at early stages of FeNTA-induced renal carcinogenesis. (A) Western blotting of renal cytoplasmic and nuclear cell fractions. Representative images and quantitative histograms of all samples assayed are shown. GAPDH and histone 3 were used as loading control for cytoplasmic and nuclear fractions, respectively. Central lane of western blot images corresponds to a HeLa cells' sample (H) used as positive control in order to confirm the identity of the bands corresponding to the proteins of interest. IκBα and EGFR levels increased in both cell fractions at both studied times in DF groups. (B) Graphs of translocation calculated by dividing the nuclear fraction RDU by total (cytoplasmic + nuclear) RDU. No statistical changes were observed. (C) Immunohistochemistry representative images of each protein assessed confirming the results obtained by the western blot assays. Magnification, x400. Bars represent the mean ± standard error of the mean. n=4 for C groups, and 5 for DF groups. *P≤0.05 vs. corresponding C. C, Control groups; DF, N-dietilnitrosamine + FeNTA treated groups; RDU, relative densitometric units vs. corresponding loading control; EGFR, epidermal growth factor receptor; H, HeLa cells' sample.

a decrease in the intensity of the band in samples from the DF group compared with that from the C one. EGFR mRNA levels, however, remained significantly heightened at both times studied (Fig. 4B).

Subcellular localization of IκBα and EGFR at early stages of FeNTA-induced renal carcinogenesis. Cytoplasmic and nuclear fractions were prepared to investigate the subcellular distribution of IκBα and EGFR by WB (Fig. 5A). For this specific determination, relative densitometric units were not adjusted to the values of the corresponding C groups, in order to facilitate the assessment of the differences in both cell fractions of the kidney cortex from C and DF treated animals. GAPDH and histone 3 were used as loading controls

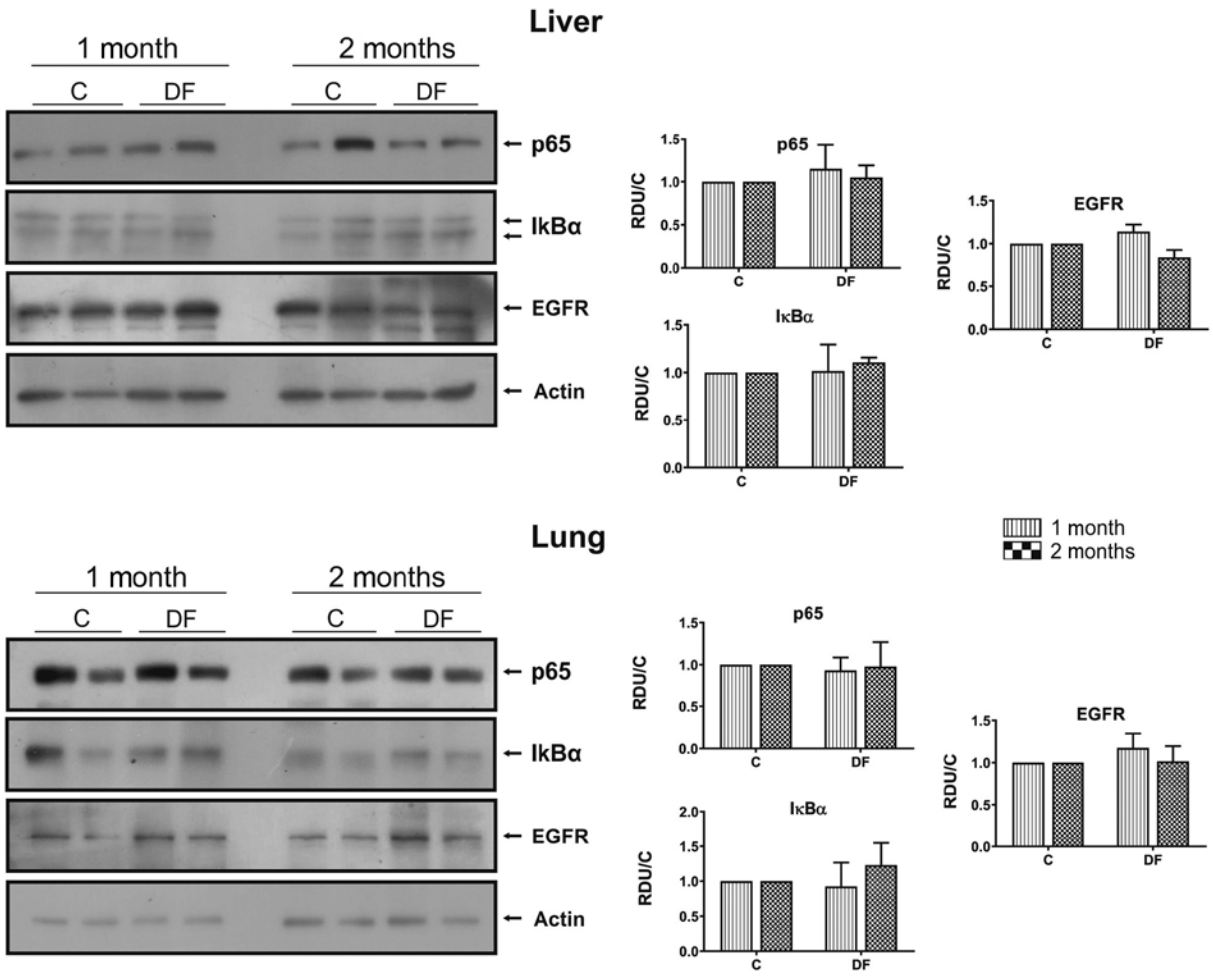

Figure 6. Liver and lung p65, IκBα and EGFR protein levels at early stages of FeNTA-induced renal carcinogenesis. Western blotting representative images and quantitative histograms are shown. No changes were observed in the expression of any of these proteins in either the liver or the lung. Bars represent the mean ± standard error of the mean. n=4 for C groups, and 5 for DF groups. P>0.05 vs. corresponding C. C, Control groups; DF, N-dietilnitrosamine + FeNTA treated groups; RDU, relative densitometric units; EGFR, epidermal growth factor receptor.

for cytoplasmic and nuclear extracts, respectively. As it can be seen, IκBα and EGFR were present in the cytoplasm as well as in the nucleus and displayed a statistically significant increase in both cell fractions, which appears to be higher after one month than after two, a behavior that coincides with that observed when total extracts were analyzed (Fig. 3). However, no changes were detected in the translocation rate of either of these proteins (Fig. 5B), calculated by dividing the nuclear fraction by the total densitometric units, though a tendency to accretion was observed in the first month. In addition, these results were corroborated by IHC (Fig. 5C), observing both proteins (IκBα and EGFR) mostly in the cytoplasm but also in the nucleus, especially IκBα.

p65, IκBα and EGFR in hepatic and lung tissues. Finally, the authors reported in a previous study (6) that no primary tumors were developed in liver or lungs using the scheme of FeNTA-exposure followed in the present investigation; thus, in order to determine if the alterations observed in p65, IκBα and EGFR behavior were particularly associated with the kidney, and was not a generalized response, the status of these proteins was determined in hepatic and lung tissues, finding no differences between C and DF groups (Fig. 6).

Discussion

RCC is the most common urological type of cancer in adults and has a high mortality rate due to several complications, such as a late diagnosis (1), which additionally makes it very difficult to study events happening at RCC's early phases, this being therefore feasible mostly in experimental models. The research group implemented a FeNTA-induced renal carcinogenesis protocol in rats and all obtained tumors were histopathologically characterized as clear cell subtype of RCC (6), the most frequent subtype in patients (1,4), and even different Fuhrman grades were identified. Also, pre-neoplastic lesions as well as different pro-carcinogenic alterations have been found after either one or two months of FeNTA-exposure and, consequently, these times of exposure were established as distinct early stages of the carcinogenesis process (5,6).

The present study found an overexpression of p65 in FeNTA-induced renal tumors, in agreement with previous observations for NF-κB in rat kidney after long term of FeNTA-exposure (36,37) and similar to what happens in patients' clear cell subtype tumors (14-16,19), as well as in some RCC human cell lines (13). Moreover, NF-κB activity is principally regulated by its inhibitory protein, IκBα, and a

substantial decrease, or even its absence, was observed in the experimental tumors, which is consistent with the findings of Oya *et al* (14) in human RCC. Also, it is worth noting that IκBα was less reduced and its nuclear presence was more frequent in NTT compared with TT and AT, suggesting that it must be restraining NF-κB activity in this area, where p65 was found to be increased in the same way as in TT, thus IκBα might be at least one of the mechanisms by which these cells are defended from malignant transformation. For its part, the mean value of EGFR levels in FeNTA-induced tumors exhibited an enhancement compared with renal tissue from C rats, despite some of them presenting no changes or even a decrease, as described in human tumors (23). Likewise, EGFR mRNA levels increased in most experimental tumors (61%), suggesting that the augment in the protein is transcriptionally induced and very probably caused, at least in part, by NF-κB, since p65 also augmented. Nevertheless, the clinical significance of the EGFR enhancement is still controversial and seems to be associated to its subcellular distribution (12,24,25,27,28). In this respect, since EGFR was found preferentially in the cytoplasm of the tumor cells, a bad prognosis would be expected according to Kankaya *et al* (25), who analyzed ccRCC subtype particularly.

Subsequently, the behavior of these molecules at early stages of renal carcinogenesis was analyzed. After one month of FeNTA-exposure, NF-κB activity was augmented even though p65 levels did not change and IκBα was increased. This could be explained by p65 posttranslational modifications which have been reported to increase the affinity of the transcription factor for its target sequence or to promote its association with some co-activators (38,39) and thus, IκBα might be playing other roles than regulating NF-κB. In this latter case, for instance, some authors have demonstrated that nuclear IκBα forms part of a transcriptional complex that associates with the promoter of different genes such as *hox* (40). Products of *hox* genes are a family of transcription factors implicated in renal organogenesis, and a change in their expression has been associated with ccRCC development (41,42). In fact, the present results showed augmented levels of IκBα in the cytoplasm but also in the nucleus and, interestingly, a tendency to increase its nuclear translocation was even noticed in the first month. On the other hand, it has been established that, besides preventing NF-κB translocation into the nucleus, IκBα is able to retain p53 in the cytoplasm, thereby counteracting the tumor-suppressive functions of p53 in other neoplasias (43). Nowadays, however, the behavior of HOX proteins and their possible role in the FeNTA-induced renal carcinogenesis are unknown and, to the best of our knowledge, the association between IκBα and p53 has not been investigated in RCC, which represent interesting perspectives for future studies.

It is likewise important to point out that exposure of rats to FeNTA during either one or two months, not only induced a renal increase of IκBα, but a shift in its electrophoretic mobility was detected, suggesting that a modified form of IκBα is accumulating in response to the carcinogen. Moreover, this shifted IκBα band increased more in the first month than at the second one. Phosphorylation of IκBα gives rise to its ubiquitination, a modification that is recognized by the 26S proteasome for the inhibitor's degradation. It may therefore indicate that the carcinogen provokes IκBα renal accumulation due to the inhibition of the 26S proteasome, effect that has been demonstrated by Okada *et al* (44). IκBα accretion may then be an early alteration that leads to promotion of the pro-carcinogenic mechanisms described above.

After two months of carcinogen exposure, in contrast, renal NF-κB activity decreased and this was consistent with the IκBα rise, suggesting that IκBα is carrying out its classical inhibitory functions on the NF-κB transcription factor at this more advanced early stage of renal carcinogenesis. Hence, the behavior observed at the first month seems to be the primary response to the carcinogen, whereas after two months, this effect is being controlled probably in most renal cells as a defense mechanism against malignant transformation, as was proposed above for NTT. However, as mentioned earlier, a shifted band of IκBα was also observed in WB assays after this time of FeNTA-exposure, so it would be relevant to identify posttranslational modifications possibly present in IκBα at the different stages of the carcinogenic process and to investigate the roles this protein might be playing in each stage. Intensive efforts are been conducted in the author's laboratory in this respect. Furthermore, a common therapeutic approach is to prevent the degradation of IκBα, but the true contribution of this protein to cancer pathogenesis is far from being understood (43).

Regarding EGFR, protein levels increased similarly after either one or two months of FeNTA exposure, as well as those of its mRNA, indicating a transcriptional regulation. Nevertheless, the increase in the receptor's protein levels was notably higher (around 25-30 times vs. C) than that of its mRNA (1.4 times vs. C), hence translational and/or posttranslational events may be involved too. Furthermore, although to a lesser extent, EGFR protein levels also increased more than its mRNA levels in the experimental tumors (2 vs. 1.4 times, respectively). EGFR, for example, may have a greater stability, as a result of a decrease in its degradation. This hypothesis is supported by Zhou and Yang (45), who demonstrated deficient EGFR degradation in human ccRCC cell lines induced by an accumulation of HIF2α, which suppress rabaptin-5 gene expression, thus delaying EGFR lysosomal degradation, since this protein mediates endosome-lysosome fusion. Results from the author's laboratory, soon to be published, also indicate an increase of HIF2α renal levels after two months of FeNTA-exposure as well as in the induced tumors. This mechanism may explain the cytoplasmic localization of EGFR found in the present study too. It is unknown, however, if this mechanism takes place in rats.

In the first month, the increase of EGFR mRNA levels coincided with the rise found in NF-κB activity, suggesting that this transcriptional factor is at least one of the causes of the receptor's response. After two months, however, while EGFR mRNA levels were still high, NF-κB's activity decreased, so the receptor's increment could be a consequence of other factors. For example, HIF2α, which aside from participating in EGFR stabilization as previously discussed, is likewise involved in EGFR gene expression and preliminary results from the authors' research group suggest an increase in the HIF2α transcription factor after two months' exposure, but not at the first one, contrary to that observed for NF-κB. Therefore, EGFR mRNA levels accretion may be the response to NF-κB's activity after one month of FeNTA-exposure and to HIF2α's activity at the second one. Another transcription

factor probably involved as well in the noticed EGFR behavior is AP-1, since there are 7 target sequences for it (c-Jun) in the gene promoter of the receptor (46) and an increase of AP-1 activity (c-Jun EMSA) at the early stages of FeNTA-induced renal carcinogenesis has been observed (still unpublished results of our group). On the other hand, although EGFR's most studied and reported function is as a cell membrane receptor transducing extracellular signals, its nuclear translocation has also been demonstrated, where it acts as a transcription co-factor linked to other proteins including STAT3, STAT5 and E2F1 (47,48), or stimulates DNA repair by associating with the catalytic subunit of DNA-dependent protein kinases when DNA is damaged (49-51). Therefore, EGFR subcellular location was determined, finding that this receptor is present and increased in the cytoplasm, but also in the nucleus after either one or two months of FeNTA-exposure, while in tumors the vast majority was in the cytoplasm. Hence, at the early stages of carcinogenesis, EGFR may be participating in renal cells' transformation by stimulating signaling pathways associated with cell proliferation, angiogenesis, invasion and apoptosis inhibition, but also may be playing anti-oncogenic roles such as DNA repair promotion as a protective mechanism against FeNTA-induced oxidative damage (52); moreover, EGFR may also be playing these anti-oncogenic roles in the non-transformed renal tissue areas (NTT and AT), where this receptor was observed in the nucleus more frequently compared with tumors. In contrast, in the neoplastic tissue, EGFR could be preferentially participating in tumor maintenance by inducing, for example, angiogenic signaling pathways, as this receptor was preferentially localized in the cytoplasm. Nevertheless, what EGFR is indeed doing at each stage of carcinogenesis should be investigated in future studies.

Finally, whether the alterations in p65, IκBα and EGFR observed in kidney were also present in liver and lungs, as it is known that FeNTA and DEN may cause hepatic and/or pulmonary damage was determined (53). Data indicated no alterations in either of these organs, so the behavior observed in p65, IκBα and EGFR is very probably kidney specific. Since the authors previously reported that, using the scheme of FeNTA-exposure followed in the present study, no primary tumors were developed in the liver or lungs (5,6), these observations strongly support the participation of the molecules analyzed in the current study in renal carcinogenesis.

It is worth pointing out that the present results, together with the great similarity with histological and mitogen associated protein kinase's behavior previously reported (5,6), reinforce the resemblance between the experimental and human renal carcinoma, and strengthen the usefulness of the experimental model to study this type of cancer, particularly in its early stages, which are almost impossible to analyze in patients.

In conclusion, according to the evidence obtained in the present work, NF-κB, IκBα and EGFR are probably implicated in the carcinogenic process, but these molecules undergo different adjustments as it evolves. In summary, a classical combination of changes was observed in tumors, suggesting that these molecules may be important for maintenance of the malignant phenotype, as has been proposed in human RCC. On the contrary, in the two early stages assessed, distinctive non-conventional combinations of changes and subcellular distributions were observed, suggesting that their behavior could be related to different signaling pathways and therefore to particular effects depending on the phase of the carcinogenic process. Given the similarity of experimental and human neoplasms, this could also happen in human carcinoma development. Therefore, novel insights were provided in the present study to continue searching for mechanisms other than the classic roles of NF-κB, IκBα and EGFR, which may be responsible for the renal cells' malignant transformation, and then to identify molecular markers that lead to an opportune detection and to develop more effective therapeutic and/or preventive strategies against RCC.

Acknowledgements

The authors would like to thank Dr Lucía Macías Rosales, (Animal Experimentation Unit, Faculty of Chemistry, National Autonomous University of Mexico), for her assistance in animal care and treatment. Also, the authors acknowledge Dr Elena Martínez-Klimova, (Department of Biology, Faculty of Chemistry, National Autonomous University of Mexico), for her contribution to the language editing of the manuscript.

Funding

The present study was supported by the Universidad Nacional Autónoma de México through Dirección General de Asuntos del Personal Académico-Programa de Apoyo a Proyectos de Investigación e Innovación Tecnológica (UNAM-DGAPA-PAPIIT; grant nos. IN227010, IN221313 and IN228716), the Consejo Nacional de Ciencia y Tecnología (CONACyT) through Fondo Sectorial de Investigación para la Educación (grant no. 284155) and the Facultad de Química through Programa de Apoyo a la Investigación y el Posgrado (PAIP; grant no. 5000-9109), given to MEIR. TPP, FAA, CVO and PCM received a fellowship from CONACyT. Also special thanks to Programa de Apoyo a los Estudios de Posgrado (PAEP) for the donation received.

Availability of data and materials

The datasets used and/or analyzed during the current study are available from the corresponding author on reasonable request.

Authors' contributions

TPP participated in the experimental design, carcinogenesis protocol execution, all the results generation, analysis and interpretation, and is a main contributor of the manuscript preparation. FAA participated in the carcinogenesis protocol execution, electrophoretic-mobility shift assay and reverse transcription-PCR techniques standardization, data analysis and interpretation, figures design, and manuscript drafting and critical revision. JDS participated in the carcinogenesis protocol execution, different techniques advising, as well as data analysis and interpretation. CVO established the carcinogenesis protocol in our laboratory and participated in western blotting results analysis and interpretation. PCM participated in the carcinogenesis protocol execution, data analysis and interpretation, figures design, and manuscript critical revision. CAMR participated in IHC technique advising,

standardization and images acquisition, processing, analysis and interpretation. DTH contributed in IHC assays execution and results generation. MEIR followed and advised throughout the project, participated in experimental conception and design, samples extraction, data analysis and interpretation, and is a main contributor of the manuscript preparation. All authors read and approved the final manuscript.

Ethics approval and consent to participate

All experiments involving animals were performed according to the Mexican Oficial Norm NOM-062-ZOO-199 and with the approval of the Institutional Committee for the Use and Care of Laboratory Animals (FQ/CICUAL/081/14). Ethical approval for the animal experiments conducted in the study was obtained non-retrospectively. In addition, tumor burden did not exceed the recommended dimensions and rats were anesthetized and sacrificed by acceptable methods.

Patient consent for publication

Not applicable.

Competing interests

The authors declare that they have no competing interests.

References

1. Makhov P, Joshi S, Ghatalia P, Kutikov A, Uzzo RG and Kolenko VM: Resistance to systemic therapies in clear cell renal cell carcinoma: Mechanisms and management strategies. Mol Cancer Ther 17: 1355-1364, 2018.
2. Peri S, Devarajan K, Yang DH, Knudson AG and Balachandran S: Meta-analysis identifies NF-κB as a therapeutic target in renal cancer. PLoS One 8: e76746, 2013.
3. Morais C, Gobe G, Johnson DW and Healy H: The emerging role of nuclear factor kappa B in renal cell carcinoma. Int J Biochem Cell Biol 43: 1537-1549, 2011.
4. Muglia VF and Prando A: Renal cell carcinoma: Histological classification and correlation with imaging findings. Radiol Bras 48: 166-174, 2015.
5. Aguilar-Alonso FA, Solano JD, Vargas-Olvera CY, Pacheco-Bernal I, Pariente-Pérez TO and Ibarra-Rubio ME: MAPKs' status at early stages of renal carcinogenesis and tumors induced by ferric nitrilotriacetate. Mol Cell Biochem 404: 161-170, 2015.
6. Vargas-Olvera CY, Sánchez-González DJ, Solano JD, Aguilar-Alonso FA, Montalvo-Muñoz F, Martínez-Martínez CM, Medina-Campos ON and Ibarra-Rubio ME: Characterization of N-diethylnitrosamine-initiated and ferric nitrilotriacetate-promoted renal cell carcinoma experimental model and effect of a tamarind seed extract against acute nephrotoxicity and carcinogenesis. Mol Cell Biochem 369: 105-117, 2012.
7. Mitchell S, Vargas J and Hoffmann A: Signaling via the NFκB system. Wiley Interdiscip Rev Syst Biol Med 8: 227-241, 2016.
8. Hayden MS and Ghosh S: Regulation of NF-κB by TNF family cytokines. Semin Immunol 26: 253-266, 2014.
9. Desterro JM, Rodriguez MS and Hay RT: SUMO-1 modification of IκBα inhibits NF-kappaB activation. Mol Cell 2: 233-239, 1998.
10. Renard P, Percherancier Y, Kroll M, Thomas D, Virelizier JL, Arenzana F and Bachelerie F: Inducible NF-kappaB activation is permitted by simultaneous degradation of nuclear IkappaBalpha. J Biol Chem 275: 15193-15199, 2000.
11. Lua J, Qayyum T, Edwards J and Roseweir AK: The prognostic role of the non-canonical nuclear factor-kappa B pathway in renal cell carcinoma patients. Urol Int 101: 190-196, 2018.
12. Meteoglu I, Erdogdu IH, Meydan N, Erkus M and Barutca S: NF-kappaB expression correlates with apoptosis and angiogenesis in clear cell renal cell carcinoma tissues. J Exp Clin Cancer Res 27: 53, 2008.
13. Morais C, Pat B, Gobe G, Johnson DW and Healy H: Pyrrolidine dithiocarbamate exerts anti-proliferative and pro-apoptotic effects in renal cell carcinoma cell lines. Nephrol Dial Transplant 21: 3377-3388, 2006.
14. Oya M, Takayanagi A, Horiguchi A, Mizuno R, Ohtsubo M, Marumo K, Shimizu N and Murai M: Increased nuclear factor-κB activation is related to the tumor development of renal cell carcinoma. Carcinogenesis 24: 377-384, 2003.
15. Sourbier C, Danilin S, Lindner V, Steger J, Rothhut S, Meyer N, Jacqmin D, Helwig JJ, Lang H and Massfelder T: Targeting the nuclear factor-κB rescue pathway has promising future in human renal cell carcinoma therapy. Cancer Res 67: 11668-11676, 2007.
16. Đorđević G, Matušan-Ilijaš K, Sinožić E, Damante G, Fabbro D, Grahovac B, Lučin K and Jonjić N: Relationship between vascular endothelial growth factor and nuclear factor-κB in renal cell tumors. Croat Med J 49: 608-617, 2008.
17. An J and Rettig MB: Epidermal growth factor receptor inhibition sensitizes renal cell carcinoma cells to the cytotoxic effects of bortezomib. Mol Cancer Ther 6: 61-69, 2007.
18. Oka D, Nishimura K, Shiba M, Nakai Y, Arai Y, Nakayama M, Takayama H, Inoue H, Okuyama A and Nonomura N: Sesquiterpene lactone parthenolide suppresses tumor growth in a xenograft model of renal cell carcinoma by inhibiting the activation of NF-kappaB. Int J Cancer 120: 2576-2581, 2007.
19. Ng KL, Yap NY, Rajandram R, Small D, Pailoor J, Ong TA, Razack AH, Wood ST, Morais C and Gobe GC: Nuclear factor-kappa B subunits and their prognostic cancer-specific survival value in renal cell carcinoma patients. Pathology 50: 511-518, 2018.
20. Thornburg NJ and Raab-Traub N: Induction of epidermal growth factor receptor expression by Epstein-barr virus latent membrane protein 1 C-terminal-activating region 1 is mediated by NF-κB p50 Homodimer/Bcl-3 complexes. J Virol 81: 12954-12961, 2007.
21. Staruschenko A, Palygin O, Ilatovskaya DV and Pavlov TS: Epidermal growth factors in the kidney and relationship to hypertension. Am J Physiol Renal Physiol 305: F12-F20, 2013.
22. Zeng F, Singh AB and Harris RC: The role of the EGF family of ligands and receptors in renal development, physiology and pathophysiology. Exp Cell Res 315: 602-610, 2009.
23. Cohen D, Lane B, Jin T, Magi-Galluzzi C, Finke J, Rini BI, Bukowski RM and Zhou M: The prognostic significance of epidermal growth factor receptor expressionin Clear-cell renal cell carcinoma: A call for standardized methods for immunohistochemical evaluation. Clin Genitourinary Cancer 5: 264-270, 2007.
24. Kallio JP, Hirvikoski P, Helin H, Kellokumpu-Lehtinen P, Luukkaala T, Tammela TL and Martikainen PM: Membranous location of EGFR immunostaining is associated with good prognosis in renal cell carcinoma. Br J Cancer 89: 1266-1269, 2003.
25. Kankaya D, Kiremitci S, Tulunay O and Baltaci S: Prognostic impact of epidermal growth factor receptor on clear cell renal cell carcinoma: Does it change with different expression patterns? Indian J Pathol Microbiol 59: 35-40, 2016.
26. Merseburger AS, Hennenlotter J, Simon P, Kruck S, Koch E, Horstmann M, Kuehs U, Küfer R, Stenzl A and Kuczyk MA: Membranous expression and prognostic implications of epidermal growth factor receptor protein in human renal cell cancer. Anticancer Res 25: 1901-1907, 2005.
27. Mock H, Sauter G, Buchholz N, Gasser TC, Bubendorf L, Waldman FM and Mihatsch MJ: Epidermal growth factor receptor expression is associated with rapid tumor cell proliferation in renal cell carcinoma. Hum Pathol 28: 1255-1259, 1997.
28. Pu YS, Huang CY, Kuo YZ, Kang WY, Liu GY, Huang AM, Yu HJ, Lai MK, Huang SP, Wu WJ, *et al*: Characterization of membranous and cytoplasmic EGFR expression in human normal renal cortex and renal cell carcinoma. J Biomed Sci 16: 82-82, 2009.
29. Athar M and Iqbal M: Ferric nitrilotriacetate promotes N-diethylnitrosamine-induced renal tumorigenesis in the rat: Implications for the involvement of oxidative stress. Carcinogenesis 19: 1133-1139, 1998.
30. Ebina Y, Okada S, Hamazaki S, Ogino F, Li JL and Midorikawa O: Nephrotoxicity and renal cell carcinoma after use of Iron- and aluminum-nitrilotriacetate complexes in Rats2. J Natl Cancer Inst 76: 107-113, 1986.
31. Jahangir T and Sultana S: Modulatory effects of shape pluchea lanceolata against chemically induced oxidative damage, hyperproliferation and Two-stage renal carcinogenesis in wistar rats. Mol Cell Biochem 291: 175-185, 2006.

32. Mendoza-Rodrıguez CA, Monroy-Mendoza MG, Morimoto S and Cerbón MA: Pro-apoptotic signals of the bcl-2 gene family in the rat uterus occurs in the night before the day of estrus and precedes ovulation. Mol Cell Endocrinol 208: 31-39, 2003.
33. Schneider CA, Rasband WS and Eliceiri KW: NIH image to ImageJ: 25 years of image analysis. Nat Methods 9: 671-675, 2012.
34. Ledeganck KJ, Boulet GA, Horvath CA, Vinckx M, Bogers JJ, Van Den Bossche R, Verpooten GA and De Winter BY: Expression of renal distal tubule transporters TRPM6 and NCC in a rat model of cyclosporine nephrotoxicity and effect of EGF treatment. Am J Physiol Renal Physiol 301: F486-F493, 2011.
35. Cai FG, Xiao JS and Ye QF: Effects of ischemic preconditioning on cyclinD1 expression during early ischemic reperfusion in rats. World J Gastroenterol 12: 2936-2940, 2006.
36. Rehman MU, Tahir M, Khan AQ, Khan R, Lateef A, Oday OH, Qamar W, Ali F and Sultana S: Chrysin suppresses renal carcinogenesis via amelioration of hyperproliferation, oxidative stress and inflammation: Plausible role of NF-κB. Toxicol Lett 216: 146-158, 2013.
37. Siddiqi A, Hasan SK, Nafees S, Rashid S, Saidullah B and Sultana S: Chemopreventive efficacy of hesperidin against chemically induced nephrotoxicity and renal carcinogenesis via amelioration of oxidative stress and modulation of multiple molecular pathways. Exp Mol Pathol 99: 641-653, 2015.
38. Christian F, Smith EL and Carmody RJ: The regulation of NF-κB subunits by phosphorylation. Cells 5: pii: E12, 2016.
39. Perkins ND: Post-translational modifications regulating the activity and function of the nuclear factor kappa B pathway. Oncogene 25: 6717-6730, 2006.
40. Espinosa L, Bigas A and Mulero MC: Novel functions of chromatin-bound IκBα in oncogenic transformation. Br J Cancer 111: 1688-1692, 2014.
41. Cantile M, Schiavo G, Franco R, Cindolo L, Procino A, D'Armiento M, Facchini G, Terracciano L, Botti G and Cillo C: Expression of lumbosacral HOX genes, crucial in kidney organogenesis, is systematically deregulated in clear cell kidney cancers. Anticancer Drugs 22: 392-401, 2011.
42. Mulero MC, Ferres-Marco D, Islam A, Margalef P, Pecoraro M, Toll A, Drechsel N, Charneco C, Davis S, Bellora N, *et al*: Chromatin-bound IκBα regulates a subset of polycomb target genes in differentiation and cancer. Cancer Cell 24: 151-166, 2013.
43. Morotti A, Crivellaro S, Panuzzo C, Carrà G, Guerrasio A and Saglio G: IκB-α: At the crossroad between oncogenic and tumor-suppressive signals. Oncol Lett 13: 531-534, 2017.
44. Okada K, Wangpoengtrakul C, Osawa T, Toyokuni S, Tanaka K and Uchida K: 4-Hydroxy-2-nonenal-mediated impairment of intracellular proteolysis during Oxidative Stress: Identification of proteasomes as target molecules. J Biol Chem 274: 23787-23793, 1999.
45. Zhou L and Yang H: The von Hippel-lindau tumor suppressor protein promotes c-Cbl-independent poly-ubiquitylation and degradation of the activated EGFR. PLoS One 6: e23936, 2011.
46. Johnson AC, Murphy BA, Matelis CM, Rubinstein Y, Piebenga EC, Akers LM, Neta G, Vinson C and Birrer M: Activator protein-1 mediates induced but not basal epidermal growth factor receptor gene expression. Mol Med 6: 17-27, 2000.
47. Brand TM, Iida M, Luthar N, Starr MM, Huppert EJ and Wheeler DL: Nuclear EGFR as a molecular target in cancer. Radiother Oncol 108: 370-377, 2013.
48. Sharmila R and Sindhu G: Evaluate the antigenotoxicity and anticancer role of β-sitosterol by determining oxidative DNA damage and the expression of phosphorylated Mitogen-activated Protein Kinases', C-fos, C-jun, and endothelial growth factor receptor. Pharmacogn Mag 13: 95-101, 2017.
49. Bandyopadhyay D, Mandal M, Adam L, Mendelsohn J and Kumar R: Physical Interaction between epidermal growth factor receptor and DNA-dependent protein kinase in mammalian cells. J Biol Chem 273: 1568-1573, 1998.
50. Goodwin JF and Knudsen KE: Beyond DNA repair: DNA-PK function in cancer. Cancer Discov 4: 1126-1139, 2014.
51. Liccardi G, Hartley JA and Hochhauser D: EGFR nuclear translocation modulates DNA repair following cisplatin and ionizing radiation treatment. Cancer Res 71: 1103-1114, 2011.
52. Toyokuni S, Mori T and Dizdaroglu M: DNA base modifications in renal chromatin of wistar rats treated with a renal carcinogen, ferric nitrilotriacetate. Int J Cancer 57: 123-128, 1994.
53. Ansar S, Iqbal M and Athar M: Nordihydroguairetic acid is a potent inhibitor of ferric-nitrilotriacetate-mediated hepatic and renal toxicity, and renal tumour promotion, in mice. Carcinogenesis 20: 599-606, 1999.